

## Article

# An Intelligent Approach to Determine Component Volume Percentages in a Symmetrical Homogeneous Three-Phase Fluid in Scaled Pipe Conditions

Abdulilah Mohammad Mayet <sup>1</sup>, Seyed Mehdi Alizadeh <sup>2</sup>, V. P. Thafasal Ijyas <sup>1</sup>,  
John William Grimaldo Guerrero <sup>3,\*</sup>, Neeraj Kumar Shukla <sup>1</sup>, Javed Khan Bhutto <sup>1</sup>,  
Ehsan Eftekhari-Zadeh <sup>4,\*</sup> and Ramy Mohammed Aiesh Qaisi <sup>5</sup>

<sup>1</sup> Electrical Engineering Department, King Khalid University, Abha 61411, Saudi Arabia; amayet@kku.edu.sa (A.M.M.); ithafasal@kku.edu.sa (V.P.T.I.); nshukla@kku.edu.sa (N.K.S.); jbhutto@kku.edu.sa (J.K.B.)

<sup>2</sup> Petroleum Engineering Department, Australian University, West Mishref 13015, Kuwait; s.alizadeh@au.edu.kw

<sup>3</sup> Department of Energy, Universidad de la Costa, Barranquilla 080001, Colombia

<sup>4</sup> Institute of Optics and Quantum Electronics, Friedrich Schiller University Jena, Max-Wien-Platz 1, 07743 Jena, Germany

<sup>5</sup> Department of Electrical and Electronics Engineering, College of Engineering, University of Jeddah, Jeddah 21589, Saudi Arabia; dgaisi@uj.edu.sa

\* Correspondence: jgrimald1@cuc.edu.co (J.W.G.G.); e.eftekhari-zadeh@uni-jena.de (E.E.-Z.)



**Citation:** Mayet, A.M.; Alizadeh, S.M.; Ijyas, V.P.T.; Grimaldo Guerrero, J.W.; Shukla, N.K.; Bhutto, J.K.; Eftekhari-Zadeh, E.; Aiesh Qaisi, R.M. An Intelligent Approach to Determine Component Volume Percentages in a Symmetrical Homogeneous Three-Phase Fluid in Scaled Pipe Conditions. *Symmetry* **2023**, *15*, 1131. <https://doi.org/10.3390/sym15061131>

Academic Editors: Qi Kang, Feng Shen, Di Wu, Jia Wang, Bin Zhou, Longsheng Duan and Shangtong Chen

Received: 26 April 2023

Revised: 16 May 2023

Accepted: 16 May 2023

Published: 23 May 2023



**Copyright:** © 2023 by the authors. Licensee MDPI, Basel, Switzerland. This article is an open access article distributed under the terms and conditions of the Creative Commons Attribution (CC BY) license (<https://creativecommons.org/licenses/by/4.0/>).

**Abstract:** Over time, the accumulation of scale within the transmission pipeline results in a decrease in the internal diameter of the pipe, leading to a decline in efficiency and energy waste. The employment of a gamma ray attenuation system that is non-invasive has been found to be a highly precise diagnostic technique for identifying volumetric percentages across various states. The most appropriate setup for simulating a volume percentage detection system through Monte Carlo N particle (MCNP) simulations involves a system consisting of two NaI detectors and dual-energy gamma sources, namely <sup>241</sup>Am and <sup>133</sup>Ba radioisotopes. A three-phase flow consisting of oil, water, and gas exhibits symmetrical homogenous flow characteristics across varying volume percentages as it traverses through scaled pipes of varying thicknesses. It is worth mentioning that there is an axial symmetry of flow inside the pipe that creates a homogenous flow pattern. In this study, the experiment involved the emission of gamma rays from one end of a pipe, with photons being absorbed by two detectors located at the other end. The resulting data included three distinct features, namely the counts under the photopeaks of <sup>241</sup>Am and <sup>133</sup>Ba from the first detector as well as the total count from the second detector. Through the implementation of a two-output MLP neural network utilising the aforementioned inputs, it is possible to accurately forecast the volumetric percentages with an RMSE of under 1.22, regardless of the thickness of the scale. The minimal error value ensures the efficacy of the proposed technique and the practicality of its implementation in the domains of petroleum and petrochemicals.

**Keywords:** three-phase; symmetrical homogenous flow; volumetric percentage; MLP neural network; scale thickness independent

## 1. Introduction

Scale deposits in oil pipelines have long been a major cause for worry in the oil and gas industry. When scale builds up within a pipeline, it may reduce the pipe's effective cross-sectional area and impede the transport of petroleum products. This factor prevents pumps and other machinery from operating at peak efficiency. Scale buildup in a pipeline that is not closely monitored may cause malfunctions, damage to machinery, higher repair costs, and decreased output. Using a control system with volume percentage detection

characteristics is helpful for progressing operations, especially when considering scalability. Gamma ray attenuation systems are used as a standard in the study of the many variables involved in a polyphase flow [1–8]. A cesium source, two sodium iodide detectors, and a test pipe were used in the experiment reported in reference [1]. The authors constructed a two-phase flow model that included stratified, bubbly, and annular zones. The RBF neural network was trained with the count data from two detectors, and it was able to accurately classify the flow regimes and forecast the volume percentages. Using GMDH artificial neural networks, Roshni et al. (2021) were able to determine flow regimes and volume percentages from unbalanced data. The great precision achieved by overloading the system with computations was used to support its implementation. A method for detecting flow regimes and volume percentages was developed by Roshani et al. (2016) using a cobalt-60 source and a NaI detector. However, the system's accuracy in identifying such parameters was constrained by the extraction of unsuitable attributes. In 2019, experts predicted the volume fraction of a stratified three-phase flow using the Jaya optimisation algorithm [4]. Sattari and his team used a cesium source, a test pipe, and two sodium iodide detectors to create a system for accurate volume percentage measurement and flow regime categorisation. The potential of GMDH neural networks for detecting transitions between flow regimes and making volume projections was investigated in a recent study [6]. The volume percentage was calculated with a high degree of accuracy in this investigation. However, it should be noted that the research had certain limitations, one of which was that the scale amount in the pipe was not included. In [7], the thickness of the scale in an oil pipeline was measured using a dual energy source composed of Cs-137 and Ba-133. They succeeded to predict scale thickness after extensive research with a RMSE under 0.22. Recent research measured the thickness of the scale in an oil pipe using a dual-energy source of Am-241 and Ba-133. After simulating an annular three-phase flow, data from two transmission detectors were used to feed photopeaks of Am-241 and Ba-133 into an RBF neural network. As indicated in reference [8], the research resulted in estimating the scale thickness with a RMSE of less than 0.09. The use of radioisotopes as a source of eternal energy has several difficulties, such as transportation difficulties and the need for specific protective equipment for workers. Several studies [9–12] show that researchers have been looking at the possibility of using X-ray tubes to determine multiphase flow characteristics in recent years. Researchers used an X-ray tube and a NaI detector to determine the regime type and volumetric fraction of two-phase flows (as recorded in reference [9]). Two multilayer perceptrons (MLPs) were trained using temporal characteristics retrieved from the detector's output signals. The study done in reference [10] focused on the analysis of three-phase flows, simulating homogeneous, annular, and stratified flow regimes at different concentrations. The results were relatively accurate after training three radial basis function (RBF) neural networks on the frequency characteristics of the incoming signals. The MCNP programme was used to simulate four different petroleum products in research [11]. The X-ray tube served as the focal point of the simulation, in which these products were mixed in pairs in varied quantities. In order to predict the volume ratio of three different items, recorded signals were supplied as inputs to MLP neural networks. Using the results for the first three items, predicting the volume ratio for the last product was simple. The presented approach proved accurate in its predictions of both product kind and quantity. However, high accuracy was difficult to achieve because of the lack of feature extraction methods. For the sake of developing new research methods, Balubaid et al. [12] looked at using wavelet transforms as a feature extraction tool. Accuracy was improved, and the computational burden was lightened as a result of this move. Building on prior research, this study aspires to provide a highly reliable diagnosis method for volume percentages. To do so, a homogeneous flow simulation was simulated on a three-phase flow system consisting of water, gas, and oil with variable volume percentages. In each simulation, the scale layer was considered using different thickness. The research set out to use a two-output MLP neural network to estimate volume fractions with high precision. To do this, we used the overall count from the second detector in addition to the count

beneath photopeaks  $^{241}\text{Am}$  and  $^{133}\text{Ba}$  from the first detector. The following are some of the contributions made by this study:

- It shows how to enhance the accuracy of the detection system.
- It is possible to obtain volumetric fraction measurements while a three-phase flow is passing through an oil pipeline in a homogenous flow regime, even in the presence of a scale layer.
- This study aims to investigate the efficacy of utilising the photopeaks of  $^{241}\text{Am}$  and  $^{133}\text{Ba}$  in the first detector as well as the total count of the second detector for the purpose of determining volume percentages.

The collection of useful features can lead to a significant reduction in computational cost.

## 2. Simulation Setup

Numerous academic works [13–16] attest to researchers' growing interest in using the MCNP algorithm for the simulation of structures employing X-ray or gamma radiation. MCNP code was used as the simulation platform to simulate the framework suggested in this research [17]. Radioisotopes  $^{133}\text{Ba}$  and  $^{241}\text{Am}$  form the backbone of our investigation. Photons from the previously described dual energy source had an energy of 59 keV and an energy of 356 keV. These photons were sent down a steel test pipe, where they were picked up by two detectors at the far end. These gamma rays emitted symmetrically from the source, and they were shaped using a shield. The two sodium iodide detectors used in this research were placed at angles of 0 and 7 degrees with respect to the theoretical horizon. Each detector measured exactly 2.54 cm  $\times$  2.54 cm. Within the test pipe itself, a homogenous flow regime was used to mimic a three-phase flow where the main phenomena took place. The aforementioned pipe was 10 cm in diameter and had a thickness of 0.5 cm. Inside this pipe was a thickness measuring instrument in the form of a  $\text{BaSO}_4$  scale with several layers. There was a 4.5 g/cm<sup>3</sup> density scale within the pipe, and it came in 0 cm, 0.5 cm, 1 cm, 1.5 cm, 2 cm, and 2.5 cm widths and heights. The pipe could carry oil, water, and gas, and the scale was located inside of it. Water, gas, and oil were all modelled in this investigation, and their densities were 1, 0.00125, and 0.826 g per cubic centimetre, respectively. In this investigation, the simulation geometry was constructed throughout the MCNP code. The experimental framework used in this research served as the basis for validating the simulations [1]. The count totals obtained by the detectors in the experimental structure and the simulated structure were compared. It seems like they got along well enough to be considered a good match. Because there were 36 volume percentages for each of the 6 values of the scale thickness, the total number of simulations was 216. From each simulation, we extracted three separate features: the original detector's count under photopeaks  $^{241}\text{Am}$  and  $^{133}\text{Ba}$  and the second detector's overall count. The 3  $\times$  216 feature matrix was used to train a neural network. The MLP neural network was trained using three introduced inputs to predict two outputs, including the volume percentages of gas and oil. In order to reduce the volume of calculations and increase the accuracy of the neural network, the volume percentage of water can be calculated separately by subtracting the volume of the two calculated products from the volume of the pipe. Figure 1 illustrates the complete structure as described. Figure 2 depicts the signals received from two detectors and extracted features.

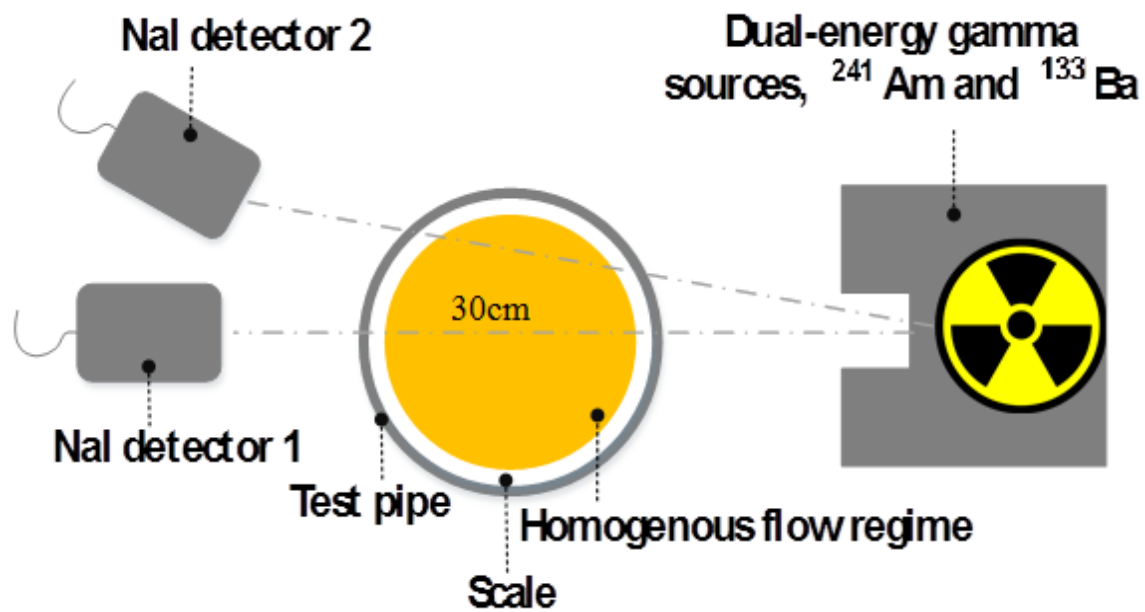


Figure 1. Implemented detection system using MCNP.

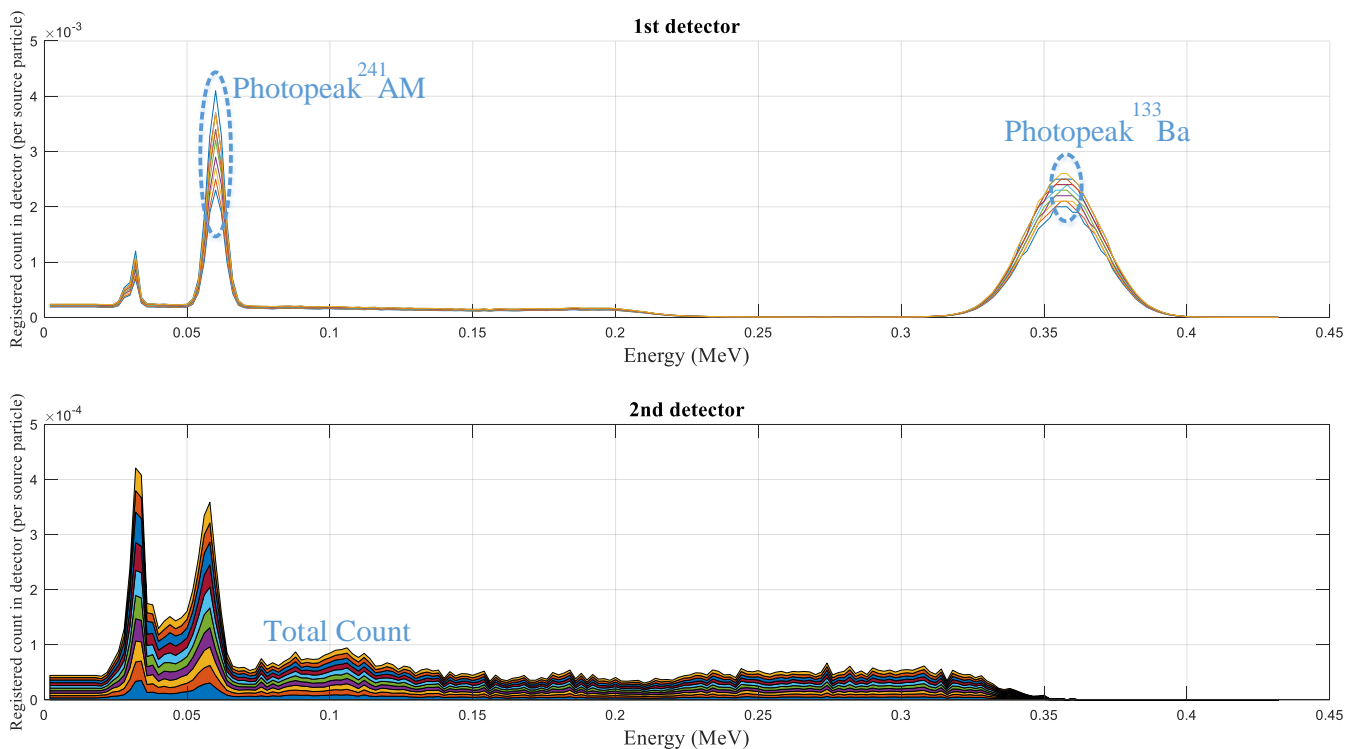


Figure 2. The extracted features of the signals that were received from both detectors.

### 3. Multilayer Perceptron Neural Network

The human brain comprises numerous interconnected neural units known as neurons, each possessing dendrites that serve as a medium for transmitting information. Upon completion of the processing stages, the axon facilitates the transfer of information from the neuron to its external environment. The aforementioned phenomena occur within the realms of physiology and biochemistry; however, the utilisation of mathematical modelling by researchers has altered the nature of the subject matter. The application of advanced mathematical techniques and artificial neural networks in various scientific domains has garnered significant interest among scholars, as evidenced by numerous studies [18–40].

The MLP neural network is widely utilised as a modelling technique. MLP neural networks were developed using the MATLAB programme (MATLAB 9.3 R2017b) that was used to extract the features listed above. Instead of using pre-made toolboxes to generate neural networks, this study meticulously hand-coded each stage of the process from training to validation to testing. Several neural network construction toolboxes may be available inside this MATLAB package. It is worth noting that the “feedforwardnet” function was used to train the neural network. The network architecture comprises three distinct components, namely the input layer, the hidden layer, and the output layer. Multiple hidden layers can be utilised in neural networks. Activation functions are executed within the hidden layers to perform mathematical operations. The determination of the quantity of layers, the quantity of neurons in the hidden layer, and the selection of the activation function are contingent upon the characteristics and extent of non-linear properties exhibited by the extant data. The output of neurons can be expressed as follows [41,42]:

$$n_l = \sum_{i=1}^u x_i w_{ij} + b \quad j = 1, 2, \dots, m \quad (1)$$

$$u_j = f \left( \sum_{i=1}^u x_i w_{ij} + b \right) \quad j = 1, 2, \dots, m \quad (2)$$

$$output = \sum_{n=1}^j (u_n w_n) + b \quad (3)$$

The input parameters are denoted by the variable  $x$ . The weighting factor, represented by  $W$ , the bias term, identified by  $b$ , and the activation function, denoted by  $f$ , are the variables of interest here. The numbers “ $i$ ” signify the input, while “ $j$ ” denotes the number of neurons in the current hidden layer. The available data is divided into three independent buckets—training, validation, and testing—to combat overfitting and under fitting. The training dataset is the primary source of information for the neural network’s observation and fitting processes. A subset of the dataset used to evaluate the success of the training process is sometimes referred to as “validation data” in discussions about data. In the testing phases of training, these data are used to put the networks to the test. Using test data is essential for verifying the accuracy of the trained neural network. To flourish in the real world, a neural network must demonstrate competence with all three types of input. To conduct the analysis, researchers used a dataset that included 152 training samples, 32 validation samples, and 32 test samples.

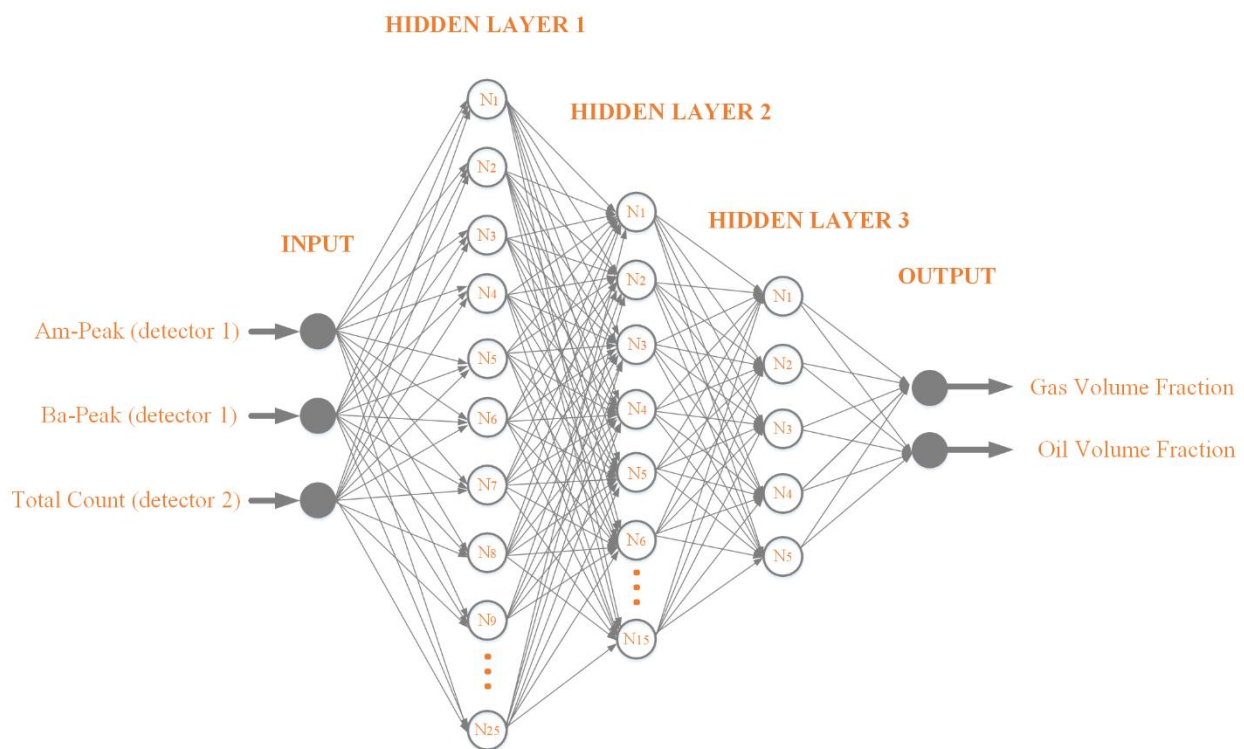
#### 4. Results

Three separate characteristics were presented in the previous sections and used as inputs to multilayer perceptron (MLP) neural networks. A matrix with 3 rows and 216 columns was considered as the input of the neural network, and a matrix with 2 rows and 216 columns was considered as the output. The two mentioned outputs are related to the volume percentage of gas and oil. Different numbers of hidden layers and neurons within those layers were used across many neural networks. The ideal framework for calculating the volumetric percentage of gas and oil is shown in Figure 3. Table 1 lists the various parameters of this network in detail. *MRE* and *RMSE* are two suggested criteria for estimating the network’s error value. Here are the equations described above that may be used as criteria:

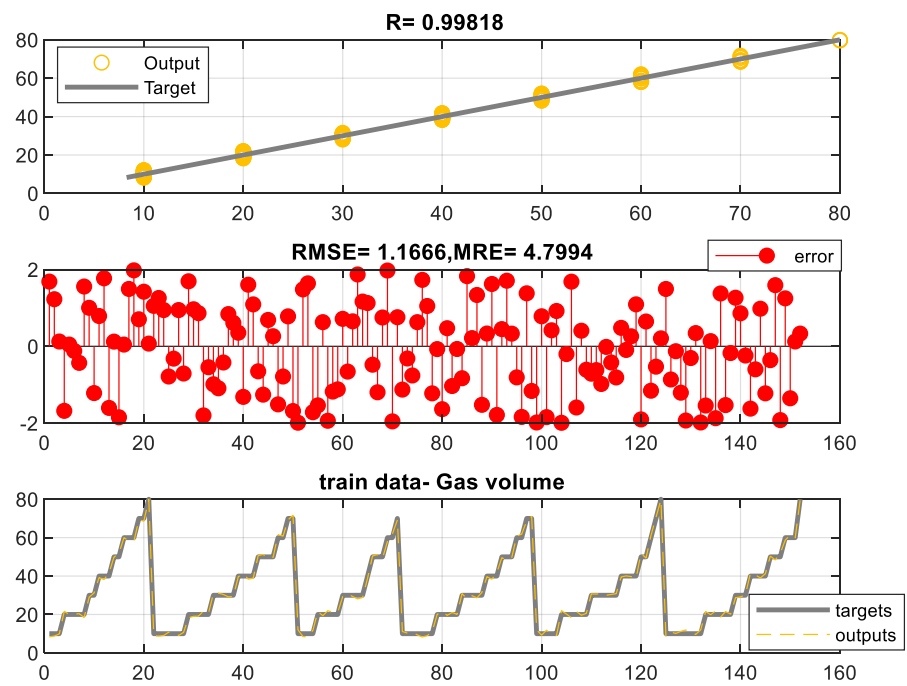
$$MRE\% = 100 \times \frac{1}{N} \sum_{j=1}^N \left| \frac{X_j(Exp) - X_j(Pred)}{X_j(Pred)} \right| \quad (4)$$

$$RMSE = \left[ \frac{\sum_{j=1}^N (X_j(Exp) - X_j(Pred))^2}{N} \right]^{0.5} \quad (5)$$

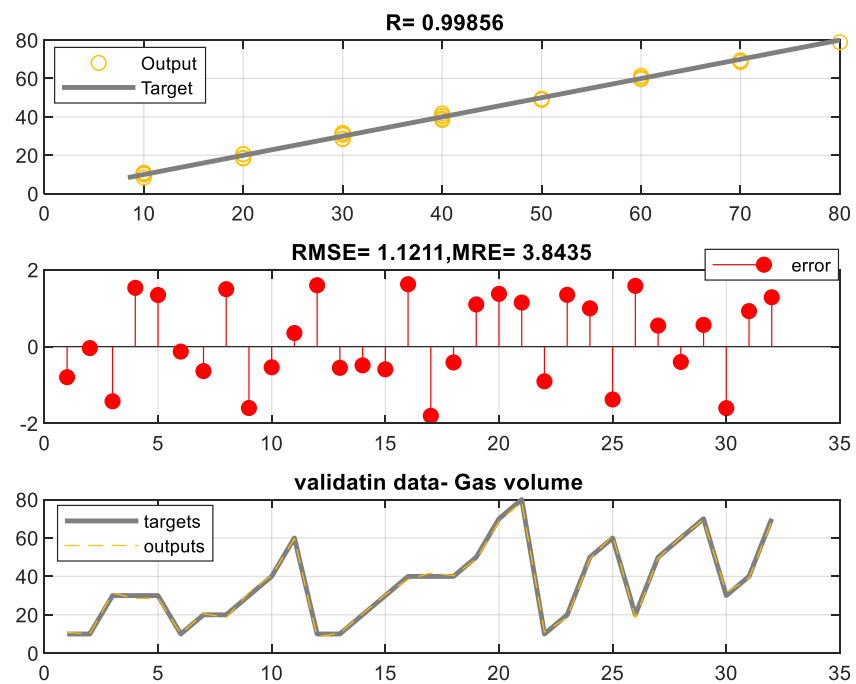
where the variable “ $N$ ” denotes the quantity of data being analysed. The terms “ $X(Exp)$ ” and “ $X(Pred)$ ” refer to the experimental and predicted values generated by the artificial neural network (ANN), respectively. Figures 4 and 5 display the regression diagram and error diagram, respectively, that show the neural networks’ responses to the three aforementioned classes. The accuracy of the network could be evaluated by comparing the goal output with the network output, which is shown together on the regression diagram. In the regression diagram, the black line represents the target outcome, while the orange circles represent the neural network’s predictions. The error diagram illustrates the deviation between the two expected outputs and the neural network’s output. In the fitting diagram, the black line represents the target output, while the orange dashed line represents the output of the network. The training, validation, and testing data used to train the neural network as well as the network’s final results are shared in Supplementary Table S1. Table 2 shows a comparison between the system presented in this research and previous studies in terms of signal processing method, type of neural network, and error rate.



**Figure 3.** MLP network for estimating gas and oil volume fractions.

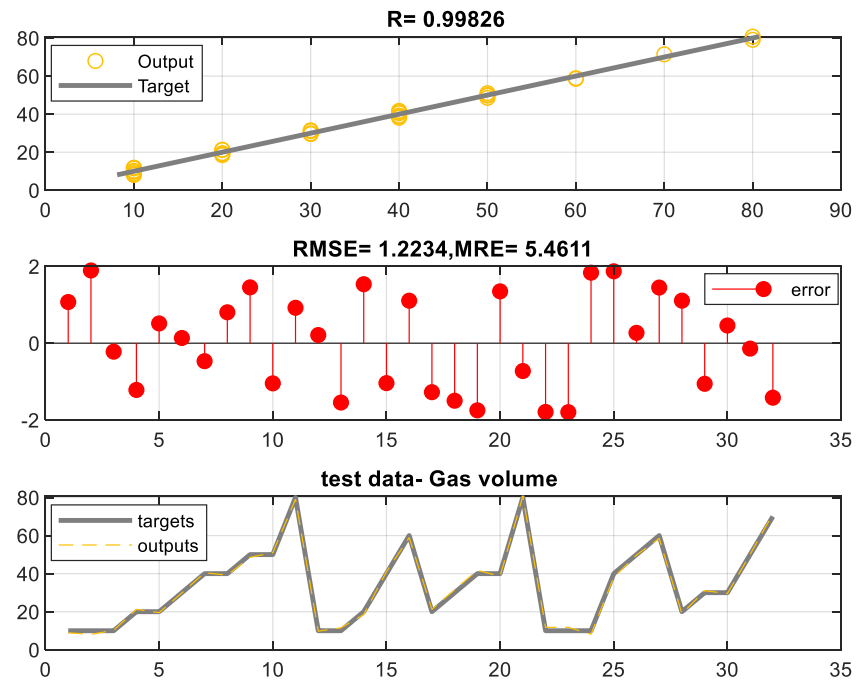


(a)



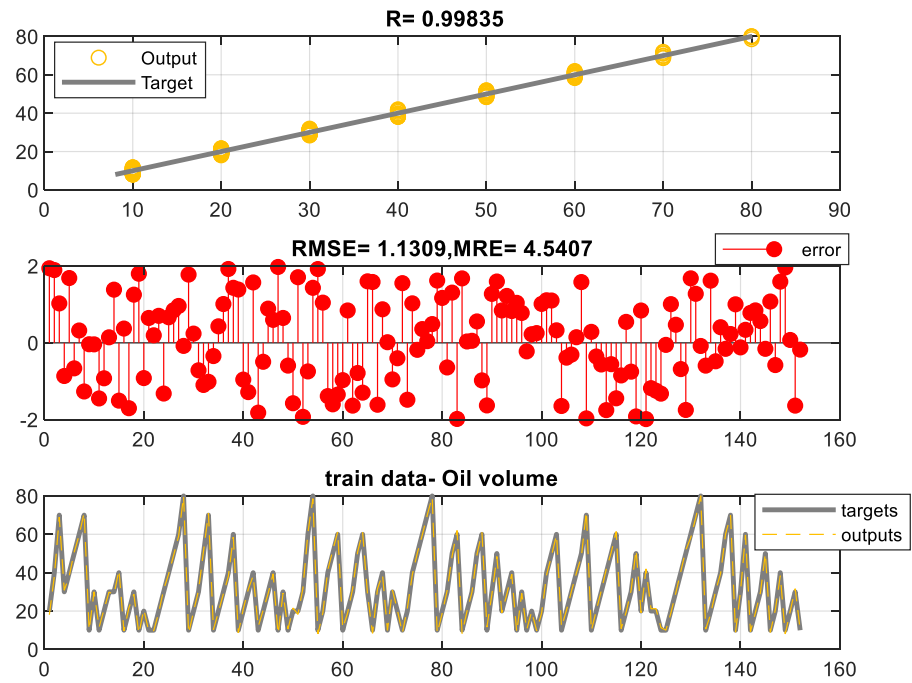
(b)

Figure 4. Cont.



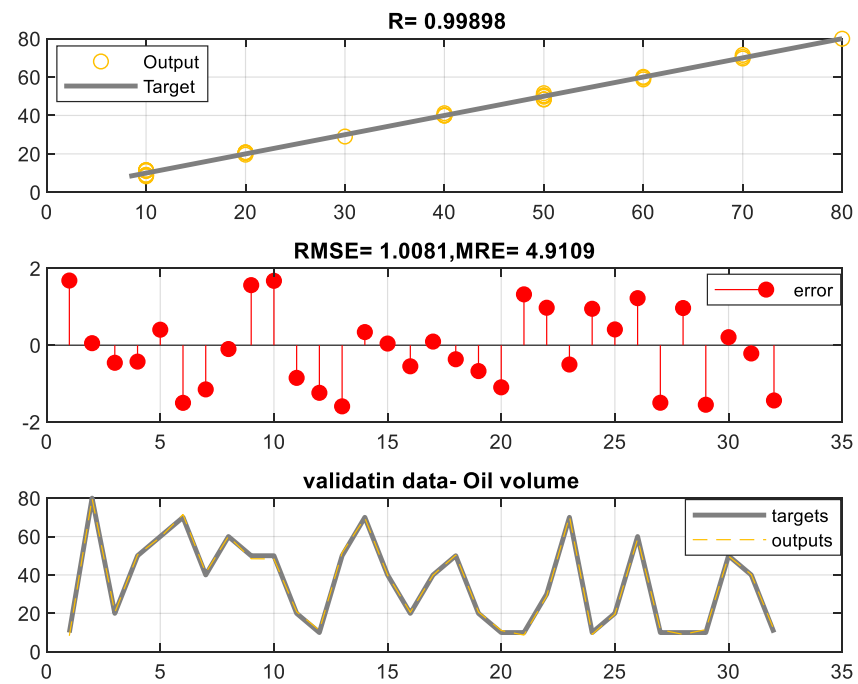
(c)

Figure 4. (a) training, (b) validation, and (c) test data sets for a neural network that predicts a percentage of gas volumes.

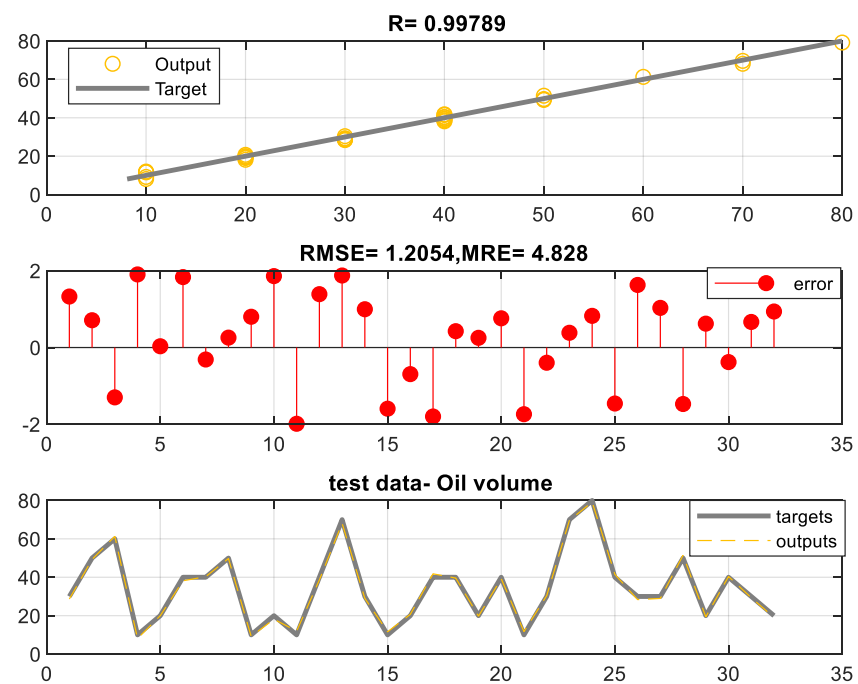


(a)

Figure 5. Cont.



(b)



(c)

**Figure 5.** (a) training, (b) validation, and (c) test data sets for a neural network that predicts a percentage of oil volumes.

**Table 1.** MLP neural network parameters for making predictions.

ANN	MLP					
Input layer neurons	3					
Neurons in the 1st hidden layer	20					
Neurons in the 2nd hidden layer	15					
Neurons in the 3rd hidden layer	5					
Neurons in the output layer	2					
Epochs	480					
Activation function	Tansig					
Output	Gas			Oil		
	<b>Train</b>	<b>Validation</b>	<b>Test</b>	<b>Train</b>	<b>Validation</b>	<b>Test</b>
RMSE	1.16	1.12	1.22	1.13	1.00	1.20
MRE%	4.79	3.84	5.46	4.54	4.91	4.82

**Table 2.** The suggested detecting system's accuracy compared to prior research.

Ref	Type of Neural Network	Extracted Features	Maximum RMSE	Maximum MSE
[1]	RBF	No feature extraction	1.29	1.66
[32]	GMDH	No feature extraction	2.71	7.34
[43]	MLP	No feature extraction	4.13	17.05
[44]	MLP	No feature extraction	1.6	2.56
[45]	RBF	Compton continuum and counts under full energy peaks of 1173 and 1333 keV	6.12	37.45
[46]	MLP	No feature extraction	2.12	4.49
[current study]	MLP	Photopeaks of $^{241}\text{Am}$ and $^{133}\text{Ba}$ in the first and total count of second detectors	1.22	1.48

Training MLP neural networks with extracted features that are relevant to the task can reduce the calculation load and improve accuracy in estimating volume percentages. Because of the system's high level of precision, the oil and petrochemical sectors did not need to use a separate detection system. Using a radioisotope source, which has been linked to negative health effects, is one possible drawback of this investigation. Therefore, it is critical that the correct safety equipment and clothing be worn at all times when working with the machinery. The absence of a source deactivation feature is evident. The minimal error achieved in this study can be attributed to the accurate processing of the acquired signals and the success of the neural network training using relevant signal features, which can compensate for any shortcomings. Future research in this area is strongly encouraged to examine numerous factors, such as temporal, frequency, and wavelet transform characteristics, and the effectiveness of various neural network models, in an effort to boost efficiency. As we mentioned previously, there is an axial symmetry of flow inside the pipe for a homogenous flow regime, and this symmetry phenomenon makes the metering process difficult. Additionally, there is a symmetrical emission of used radioisotopes. While using the presented method in this paper in the presence of these difficulties, the desired output was obtained. Figure 6 depicts the overarching procedure of the provided approach for calculating the volume fraction. In the initial phase of the detection system's architecture, as seen in the figure, the MCNP code simulated

the flows moving through the pipe and the varying thicknesses of the scale within the pipe and labeled the signals received by the detectors. The data from each simulation's received signals were then analysed to find three features: the  $^{241}\text{Am}$  and  $^{133}\text{Ba}$  photopeaks from the first detector as well as the total count from the second detector. In fact, the characteristics used in this study have been used in previous studies to determine other parameters of multiphase flows [45,46]. In this research, the performance of the mentioned characteristics to determine volume percentages in three-phase flows in the homogeneous regime and in the presence of the scale layer has been investigated. The high accuracy of the proposed method confirms the proposed characteristics in determining volume percentages. The percentages of oil and gas inside the pipe might then be predicted using the acquired features as inputs to a multi-layer perceptron neural network. Following training, the neural network's output was checked against the target output to make sure it was producing the expected results.

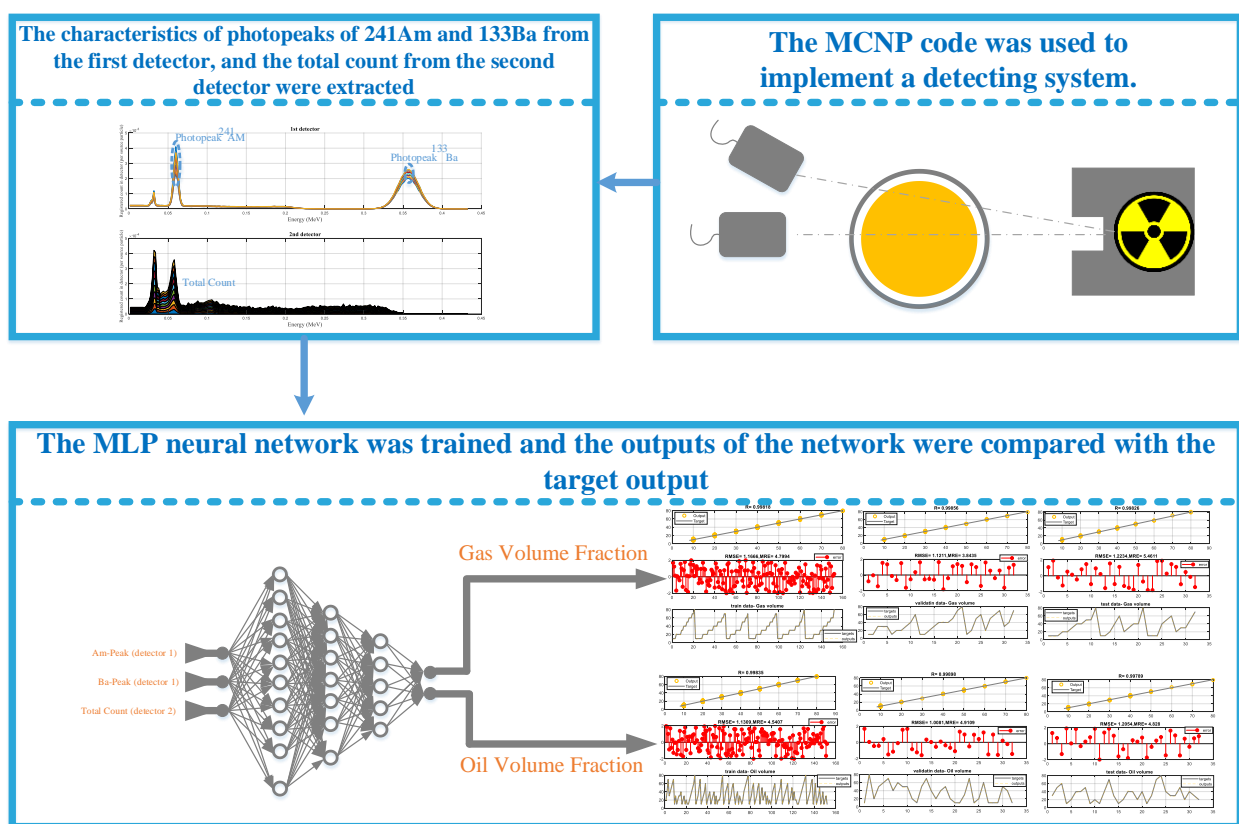


**Figure 6.** The overall process of the proposed method for measuring volume fractions within the pipe.

## 5. Conclusions

The efficiency of the oil industry may be improved by calculating the volume percentage of each passing phase of condensate inside the oil pipe. Therefore, developing and deploying a system to identify volume percentages might prove to be a helpful tool in tackling the challenges experienced in the oil business. In the present study, the gamma ray attenuation technique was employed to precisely calculate the volumetric proportion of three-phase condensates in a homogenous flow regime. The study was successful because it provided the most effective strategy for achieving the desired effect. The detecting system consists of a dual-energy gamma generator and two NaI detectors, one on either end of the pipe, to determine the relative volume of each phase. The MCNP algorithm is used to replicate the aforementioned procedure. In this study, a homogenous three-phase flow was simulated with volumes ranging from 10% to 80%. The study also investigated a range of scale thicknesses from zero centimetres to two and a half centimetres. From the signals

produced in all simulations, three characteristics were collected for this study: the count beneath Photopeaks  $^{241}\text{Am}$  and  $^{133}\text{Ba}$  of the first detector and the overall count of the second detector. These characteristics were then used in the formation of a neural network. One MLP neural network was trained using the aforementioned characteristics as inputs, and the outputs of the neural network were the gas and oil volumes as percentages. Subtracting the amounts of oil and gas from the total volume of the pipe yields an accurate estimate of the water phase's contribution to the pipe's volume. The neural network's promising performance in predicting the volume percentage with an RMSE of less than 1.22 stands out when compared to other studies. The suggested method's excellent accuracy is attributable to its skillful feature extraction and subsequent use in training neural networks, which pave the way for the construction of optimal networks. The current study introduces a detection method that has been found to be highly useful and is strongly suggested for use in the oil and petroleum sectors.

**Supplementary Materials:** The following supporting information can be downloaded at: <https://www.mdpi.com/article/10.3390/sym15061131/s1>, Table S1. The target data and the trained neural network's output for three categories of training, validation and testing.

**Author Contributions:** Methodology, A.M.M., V.P.T.I., N.K.S., J.K.B. and R.M.A.Q.; Investigation, S.M.A., J.W.G.G., A.M.M., V.P.T.I., N.K.S., J.K.B. and R.M.A.Q.; Writing—original draft, E.E.-Z.; Funding acquisition, E.E.-Z. and A.M.M. All authors have read and agreed to the published version of the manuscript.

**Funding:** The authors extend their appreciation to the Deanship of Scientific Research at King Khalid University for funding this work through large group Research Project under grant number RGP2/39/44. We acknowledge support by the German Research Foundation Projekt-Nr. 512648189 and the Open Access Publication Fund of the Thueringer Universitaets- und Landesbibliothek Jena.

**Data Availability Statement:** The data presented in this study are available on request from the corresponding author.

**Conflicts of Interest:** The authors declare no conflict of interest.

## References

1. Nazemi, E.; Roshani, G.H.; Feghhi, S.A.H.; Setayeshi, S.; Zadeh, E.E.; Fatehi, A. Optimization of a method for identifying the flow regime and measuring void fraction in a broad beam gamma-ray attenuation technique. *Int. J. Hydrogen Energy* **2016**, *41*, 7438–7444. [[CrossRef](#)]
2. Roshani, M.; Phan, G.; Roshani, G.H.; Hanus, R.; Nazemi, B.; Corniani, E.; Nazemi, E. Combination of X-ray tube and GMDH neural network as a nondestructive and potential technique for measuring characteristics of gas-oil-water three phase flows. *Measurement* **2021**, *168*, 108427. [[CrossRef](#)]
3. Roshani, G.H.; Nazemi, E.; Feghhi, S.A.H. Investigation of using  $^{60}\text{Co}$  source and one detector for determining the flow regime and void fraction in gas-liquid two-phase flows. *Flow Meas. Instrum.* **2016**, *50*, 73–79. [[CrossRef](#)]
4. Roshani, G.H.; Karami, A.; Nazemi, E. An intelligent integrated approach of Jaya optimization algorithm and neuro-fuzzy network to model the stratified three-phase flow of gas-oil-water. *Comput. Appl. Math.* **2019**, *38*, 5. [[CrossRef](#)]
5. Sattari, M.A.; Roshani, G.H.; Hanus, R.; Nazemi, E. Applicability of time-domain feature extraction methods and artificial intelligence in two-phase flow meters based on gamma-ray absorption technique. *Measurement* **2021**, *168*, 108474. [[CrossRef](#)]
6. Sattari, M.A.; Roshani, G.H.; Hanus, R. Improving the structure of two-phase flow meter using feature extraction and GMDH neural network. *Radiat. Phys. Chem.* **2020**, *171*, 108725. [[CrossRef](#)]
7. Alamoudi, M.; Sattari, M.A.; Balubaid, M.; Eftekhari-Zadeh, E.; Nazemi, E.; Taylan, O.; Kalmoun, E.M. Application of Gamma Attenuation Technique and Artificial Intelligence to Detect Scale Thickness in Pipelines in Which Two-Phase Flows with Different Flow Regimes and Void Fractions Exist. *Symmetry* **2021**, *13*, 1198. [[CrossRef](#)]
8. Taylan, O.; Abusurrah, M.; Amiri, S.; Nazemi, E.; Eftekhari-Zadeh, E.; Roshani, G.H. Proposing an Intelligent Dual-Energy Radiation-Based System for Metering Scale Layer Thickness in Oil Pipelines Containing an Annular Regime of Three-Phase Flow. *Mathematics* **2021**, *9*, 2391. [[CrossRef](#)]
9. Basahel, A.; Sattari, M.A.; Taylan, O.; Nazemi, E. Application of Feature Extraction and Artificial Intelligence Techniques for Increasing the Accuracy of X-ray Radiation Based Two Phase Flow Meter. *Mathematics* **2021**, *9*, 1227. [[CrossRef](#)]
10. Taylan, O.; Sattari, M.A.; Elhachfi Essoussi, I.; Nazemi, E. Frequency Domain Feature Extraction Investigation to Increase the Accuracy of an Intelligent Nondestructive System for Volume Fraction and Regime Determination of Gas-Water-Oil Three-Phase Flows. *Mathematics* **2021**, *9*, 2091. [[CrossRef](#)]

11. Roshani, G.H.; Ali, P.J.M.; Mohammed, S.; Hanus, R.; Abdulkareem, L.; Alanezi, A.A.; Kalmoun, E.M. Simulation Study of Utilizing X-ray Tube in Monitoring Systems of Liquid Petroleum Products. *Processes* **2021**, *9*, 828. [[CrossRef](#)]
12. Balubaid, M.; Sattari, M.A.; Taylan, O.; Bakhsh, A.A.; Nazemi, E. Applications of Discrete Wavelet Transform for Feature Extraction to Increase the Accuracy of Monitoring Systems of Liquid Petroleum Products. *Mathematics* **2021**, *9*, 3215. [[CrossRef](#)]
13. Hosseini, S.; Taylan, O.; Abusurrah, M.; Akilan, T.; Nazemi, E.; Eftekhari-Zadeh, E.; Roshani, G.H. Application of Wavelet Feature Extraction and Artificial Neural Networks for Improving the Performance of Gas–Liquid Two-Phase Flow Meters Used in Oil and Petrochemical Industries. *Polymers* **2021**, *13*, 3647. [[CrossRef](#)] [[PubMed](#)]
14. Sattari, M.A.; Korani, N.; Hanus, R.; Roshani, G.H.; Nazemi, E. Improving the performance of gamma radiation based two phase flow meters using optimal time characteristics of the detector output signal extraction. *J. Nucl. Sci. Technol. (IonSat)* **2020**, *41*, 42–54.
15. Iliyasu, A.M.; Mayet, A.M.; Hanus, R.; El-Latif, A.A.A.; Salama, A.S. Employing GMDH-Type Neural Network and Signal Frequency Feature Extraction Approaches for Detection of Scale Thickness inside Oil Pipelines. *Energies* **2022**, *15*, 4500. [[CrossRef](#)]
16. Mayet, A.M.; Salama, A.S.; Alizadeh, S.M.; Nesic, S.; Guerrero, J.W.G.; Eftekhari-Zadeh, E.; Nazemi, E.; Iliyasu, A.M. Applying Data Mining and Artificial Intelligence Techniques for High Precision Measuring of the Two-Phase Flow's Characteristics Independent of the Pipe's Scale Layer. *Electronics* **2022**, *11*, 459. [[CrossRef](#)]
17. Pelowitz, D.B. *MCNP-X TM User's Manual*; Version 2.5.0; LA-CP-05e0369; Los Alamos National Laboratory: Los Alamos, NM, USA, 2005.
18. Roshani, S.; Roshani, S. Design of a compact LPF and a miniaturized Wilkinson power divider using aperiodic stubs with harmonic suppression for wireless applications. *Wirel. Netw.* **2020**, *26*, 1493–1501. [[CrossRef](#)]
19. Hookari, M.; Roshani, S.; Roshani, S. Design of a low pass filter using rhombus-shaped resonators with an analytical equivalent circuit. *Turk. J. Electr. Eng. Comput. Sci.* **2020**, *28*, 865–874. [[CrossRef](#)]
20. Roshani, S.; Azizian, J.; Roshani, S.; Jamshidi, M.B.; Parandin, F. Design of a miniaturized branch line microstrip coupler with a simple structure using artificial neural network. *Frequenz* **2022**, *76*, 255–263. [[CrossRef](#)]
21. Lalbakhsh, A.; Mohamadpour, G.; Roshani, S.; Ami, M.; Roshani, S.; Sayem, A.S.; Alibakhshikenari, M.; Koziel, S. *Design of a Compact Planar Transmission Line for Miniaturized Rat-Race Coupler with Harmonics Suppression*; IEEE Access: Piscataway, NJ, USA, 2021; Volume 9, pp. 129207–129217.
22. Khaleghi, M.; Salimi, J.; Farhangi, V.; Moradi, M.J.; Karakouzian, M. Evaluating the behaviour of centrally perforated unreinforced masonry walls: Applications of numerical analysis, machine learning, and stochastic methods. *Ain Shams Eng. J.* **2022**, *13*, 101631. [[CrossRef](#)]
23. Moradi, N.; Tavana, M.H.; Habibi, M.R.; Amiri, M.; Moradi, M.J.; Farhangi, V. Predicting the Compressive Strength of Concrete Containing Binary Supplementary Cementitious Material Using Machine Learning Approach. *Materials* **2022**, *15*, 5336. [[CrossRef](#)] [[PubMed](#)]
24. Hanus, R.; Zych, M.; Golijanek-Jędrzejczyk, A. Measurements of Dispersed Phase Velocity in Two-Phase Flows in Pipelines Using Gamma-Absorption Technique and Phase of the Cross-Spectral Density Function. *Energies* **2022**, *15*, 9526. [[CrossRef](#)]
25. Hanus, R.; Zych, M.; Golijanek-Jędrzejczyk, A. Investigation of liquid–gas flow in a horizontal pipeline using gamma-ray technique and modified cross-correlation. *Energies* **2022**, *15*, 5848. [[CrossRef](#)]
26. Mayet, A.; Hussain, M. Amorphous W<sub>Nx</sub> Metal For Accelerometers and Gyroscope. In Proceedings of the MRS Fall Meeting, Boston, MA, USA, 30 November–5 December 2014.
27. Mayet, A.; Hussain, A.; Hussain, M. Three-terminal nanoelectromechanical switch based on tungsten nitride—An amorphous metallic material. *Nanotechnology* **2016**, *27*, 035202. [[CrossRef](#)]
28. Roshani, G.H.; Hanus, R.; Khazaei, A.; Zych, M.; Nazemi, E.; Mosorov, V. Density and velocity determination for single-phase flow based on radiotracer technique and neural networks. *Flow Meas. Instrum.* **2018**, *61*, 9–14. [[CrossRef](#)]
29. Roshani, G.H.; Nazemi, E.; Roshani, M.M. Intelligent recognition of gas-oil-water three-phase flow regime and determination of volume fraction using radial basis function. *Flow Meas. Instrum.* **2017**, *54*, 39–45. [[CrossRef](#)]
30. Roshani, G.H.; Roshani, S.; Nazemi, E.; Roshani, S. Online measuring density of oil products in annular regime of gas-liquid two phase flows. *Measurement* **2018**, *129*, 296–301. [[CrossRef](#)]
31. Nazemi, E.; Feghhi, S.A.H.; Roshani, G.H.; Peyvandi, R.G.; Setayeshi, S. Precise void fraction measurement in two-phase flows independent of the flow regime using gamma-ray attenuation. *Nucl. Eng. Technol.* **2016**, *48*, 64–71. [[CrossRef](#)]
32. Roshani, M.; Sattari, M.A.; Ali, P.J.M.; Roshani, G.H.; Nazemi, B.; Corniani, E.; Nazemi, E. Application of GMDH neural network technique to improve measuring precision of a simplified photon attenuation based two-phase flowmeter. *Flow Meas. Instrum.* **2020**, *75*, 101804. [[CrossRef](#)]
33. Ahmad, M.; Alfayad, M.; Aftab, S.; Khan, M.; Fatima, A.; Shoab, B.; Daoud, M.; Sabri, N. Data and Machine Learning Fusion Architecture for Cardiovascular Disease Prediction. *Comput. Mater. Contin.* **2021**, *69*, 2717–2731. [[CrossRef](#)]
34. Daoud, M.; Aftab, S.; Ahmad, M.; Khan, M.; Iqbal, A.; Abbas, S.; Iqbal, M.; Ihnaini, B. Machine Learning Empowered Software Defect Prediction System. *Intell. Autom. Soft Comput.* **2021**, *31*, 1287–1300. [[CrossRef](#)]
35. Daoud, M.S.; Ayes, A.; Al-Fayoumi, M.; Hopgood, A.A. Location Prediction Based on a Sector Snapshot for Location-Based Services. *J. Netw. Syst. Manag.* **2014**, *22*, 23–49. [[CrossRef](#)]
36. Shehab, M.; Abualigah, L.; Jarrah, M.I.; Alomari, O.A.; Daoud, M.S. (AIAM2019) Artificial Intelligence in Software Engineering and inverse: Review. *Int. J. Comput. Integr. Manuf.* **2020**, *33*, 1129–1144. [[CrossRef](#)]

37. Golijaneck-Jędrzejczyk, A.; Mrowiec, A.; Kleszcz, S.; Hanus, R.; Zych, M.; Jaszczur, M. A numerical and experimental analysis of multi-hole orifice in turbulent flow. *Measurement* **2022**, *193*, 110910. [[CrossRef](#)]
38. Abidi, W.U.; Daoud, M.S.; Ihnaini, B.; Khan, M.A.; Alyas, T.; Fatima, A.; Ahmad, M. Real-Time Shill Bidding Fraud Detection Empowered With Fussed Machine Learning. *IEEE Access* **2021**, *9*, 113612–113621. [[CrossRef](#)]
39. Jedkare, E.; Shama, F.; Sattari, M.A. Compact Wilkinson power divider with multi-harmonics suppression. *AEU-Int. J. Electron. Commun.* **2020**, *127*, 153436. [[CrossRef](#)]
40. Taylor, J.G. *Neural Networks and Their Applications*; John Wiley & Sons Ltd.: Brighton, UK, 1996.
41. Gallant, A.R.; White, H. On learning the derivatives of an unknown mapping with multilayer feedforward networks. *Neural Netw.* **1992**, *5*, e129–e138. [[CrossRef](#)]
42. Roshani, M.; Ali, P.J.; Roshani, G.H.; Nazemi, B.; Corniani, E.; Phan, N.H.; Tran, H.N.; Nazemi, E. X-ray tube with artificial neural network model as a promising alternative for radioisotope source in radiation based two phase flowmeters. *Appl. Radiat. Isot.* **2020**, *164*, 109255. [[CrossRef](#)] [[PubMed](#)]
43. Peyvandi, R.G.; Rad, S.I. Application of artificial neural networks for the prediction of volume fraction using spectra of gamma rays backscattered by three-phase flows. *Eur. Phys. J. Plus* **2017**, *132*, 511. [[CrossRef](#)]
44. Roshani Gholam, H.; Nazemi Ehsan Shama Farzin, A.; Mohammad, I.; Salar, M. Designing a simple ra-diometric system to predict void fraction percentage independent of flow pattern using radial basis function. *Metrol. Meas. Syst.* **2018**, *25*, 347–358.
45. Mayet, A.M.; Chen, T.C.; Alizadeh, S.M.; Al-Qahtani, A.A.; Qaisi, R.M.A.; Alhashim, H.H.; Eftekhari-Zadeh, E. Application of Artificial Intelligence for Determining the Volume Percentages of a Stratified Regime's Three-Phase Flow, Independent of the Oil Pipeline's Scale Thickness. *Processes* **2022**, *10*, 1996. [[CrossRef](#)]
46. Mayet, A.M.; Chen, T.C.; Ahmad, I.; Tag Eldin, E.; Al-Qahtani, A.A.; Narozhnyy, I.M.; Alhashim, H.H. Application of neural network and dual-energy radiation-based detection techniques to measure scale layer thickness in oil pipelines containing a stratified regime of three-phase flow. *Mathematics* **2022**, *10*, 3544. [[CrossRef](#)]

**Disclaimer/Publisher's Note:** The statements, opinions and data contained in all publications are solely those of the individual author(s) and contributor(s) and not of MDPI and/or the editor(s). MDPI and/or the editor(s) disclaim responsibility for any injury to people or property resulting from any ideas, methods, instructions or products referred to in the content.